A Wireless Power Transfer System with Inverse Coupled Current Doubler Rectifier for HighOutput Current Applications

L. Shi, A. Delgado, R. Ramos and P. Alou

A Wireless Power Transfer System with Inverse Coupled Current Doubler Rectifier for High Output Current Applications

Lixin Shi, *Student Member*,*IEEE*, Alberto Delgado, *Student Member*, *IEEE*, Regina Ramos, *Student Member*, *IEEE*, and Pedro Alou, *Member*, *IEEE*

***Abstract*—In this paper, a series-series wireless power transfer (WPT) system combined with an inverse coupled current doubler rectifier (ICCDR) is proposed, as a very appropriate WPT topology for high current applications. The ICCDR uses an autotransformer to reduce the losses on the rectifier stage, which is suitable for high current low voltage output applications. Furthermore, a comprehensive comparison between the proposed WPT system with ICCDR and the traditional WPT system with full bridge rectifier is presented. In the proposed WPT system, the primary parameter configuration and circuit behavior keep the same, while the secondary side altered, contributing to a volume reduction on the resonant capacitor. The system overall efficiency and power density are improved significantly. Accordingly, a 10kW 400V/48V WPT prototype for battery charging is constructed and tested to validate this proposal. The output voltage is in the range between 38 Vdc and 55 Vdc, and the rated output current is 200A. The overall efficiency of the proposed system reaches 94%, improving 2% efficiency with 220W energy saving with respect to the traditional diode-rectifier system, when 9.5kW output power is delivered. Theoretical analysis and experimental results have verified that the proposed system shows great advantages in high power WPT applications.**

***Index Terms*—DC-DC power converter, wireless power transfer (WPT), inverse coupled current doubler rectifier, high output current.**

I. Introduction

RECENTLY, wireless power transfer (WPT) has been widely used in various application fields [1] – [7] such as biomedical implants, portable mobile devices, mart cordless kitchen appliances, and electric vehicle (EV) charging, where the power levels of the system range from a few milliwatts up to several kilowatts.

The overall efficiency of WPT systems is one of the most critical performance, especially for high-power applications [7]. The main sources of losses in a high power WPT system are coming from the inverter stage, the resonant coil link, and the rectifier stage. Many papers have been published to maximize the efficiency and reduce the losses. In [8] – [11], different inverter topologies have been studied to improve the efficiency. In [8], a current-fed parallel resonant push-pull inverter is proposed for WPT to reduce the conduction losses on the switches. Various combinations of compensation topologies (series or parallel) have been investigated in [12] – [15] to improve coil link efficiency. High-order resonant circuits such as LCC are also investigated particularly for dynamic charging of electric vehicles [16], [17]. In [18], a method that controls the phase shift of active rectifiers to modify the load impedance is proposed to improve the system overall efficiency.

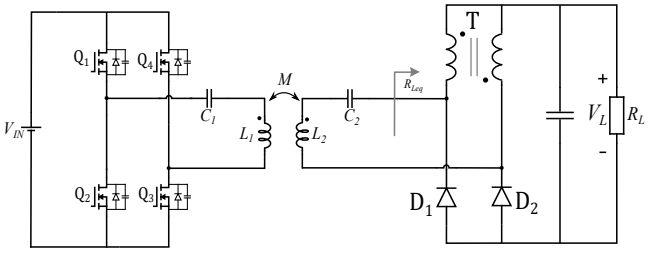

Fig. 1. Proposed solution for high current WPT converters.

Battery charging applications typically require relatively low voltages and high output currents, which leads to large conduction losses on the rectifier stage. The energy lost on the rectifier passes though the inverter and coil link causing additional losses on these two stages. Therefore, decreasing the losses on the rectifier can not only improve the efficiency of the rectifier but also can reduce the losses on the inverter and coil link. Designing an efficient rectifier is gaining more attractive.

It is well known that current doubler rectifier (CDR) is very suitable for low voltage and high current applications. Because the secondary current is half of the output current, making it possible to reduce conduction losses in high current applications [19] – [24]. This type of rectifier was mainly used in push-pull stages and full-bridge or half-bridge converters [23]. However, it cannot be directly used to a series-series (S-S) WPT system, because the S-S WPT system is injecting a resonant ac current into the rectifier, being necessary that the rectifier presents a voltage source behavior in the ac

Manuscript received December 26, 2020; revised March 28, 2021; accepted April 24, 2021.

The authors are with the Centro de Electrónica Industrial, Universidad Politécnica de Madrid (UPM), 28006 Madrid, Spain (e-mail: lixin.shi@upm.es; a.delgado@upm.es; regina.ramos@upm.es; pedro.alou@upm.es;).

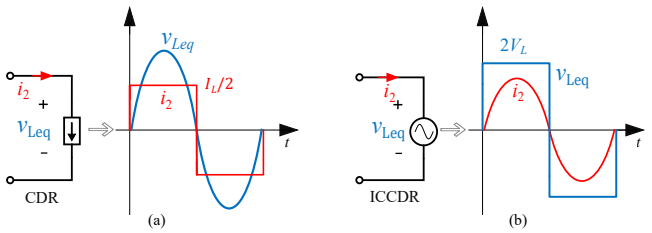

Fig. 2. Main waveforms comparison of traditional CDR and the ICCDR. (a) Traditional CDR. (b) The ICCDR.

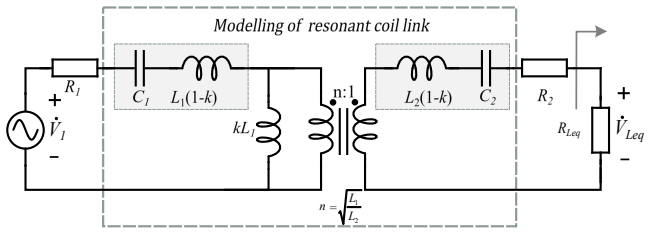

Fig. 3. Equivalent circuit of a S-S resonant WPT converter.

side. However, the CDR behaves like an ac current source in the ac side, which is not compatible with S-S WPT system. Therefore, it is necessary to have a capacitor in parallel at the input of the CDR to decouple both current sources as in [25] and [26].

In [27] and [28], an inverse coupled current double rectifier (ICCDR) for LLC resonant converters is proposed, which is also compatible in the S-S WPT system. The main contribution of this paper is the analysis of using the ICCDR in S-S WPT systems (Fig. 1). The ICCDR uses an autotransformer instead of the two independent inductors in the CDRs, it keeps the same performance to double the current as CDRs; Fig. 2 shows the voltage and current waveforms of the CDR and the ICCDR. The current is square, and voltage is sinusoidal in the traditional CDR as shown in Fig. 2 (a), which makes the CDR not compatible with S-S WPT system. In contrast, as shown in Fig. 2 (b), the current through the ICCDR keeps sinusoidal and the voltage is squared, behaving like an ac voltage source, being fully compatible with the S-S WPT system without being necessary to add any capacitance as in [25] and [26]. Compared with the CDR, the size of magnetic components in the ICCDR is smaller, because the two independent inductors in the CDR store energy while the autotransformer (inverse couple inductors) of the ICCDR does not store energy, being very suitable in high current applications. Besides, the CDR requires a parallel capacitor at the input to be compatible with the S-S WPT system, making the equivalent ac load to be capacitive, the equivalent reactance of the load stage will depend on the output power, which makes the secondary harder to tune with load variation. However, the equivalent ac impedance of the ICCDR is pure resistive under the whole power range.

Compared with the full bridge rectifier WPT system, the losses on the ICCDR can be reduced dramatically for low voltage high output current applications (200A). Besides, the volume and weight of secondary can be minimized dramatically due to the volume save of secondary resonant capacitors. A comprehensive comparison between the proposed ICCDR system and the traditional full bridge rectifier system is presented in this paper. The effect of the added ICCDR to the WPT system is described and verified by simulation and measurements.

This paper is organized as follows: Section II analyzes the operating principles of the proposed WPT system based on the fundamental harmonic analysis model. In Section III, a comprehensive comparison between the proposed ICCDR system and the traditional diode-rectifier system is presented. In Section IV, a 10kW 400V/48V WPT prototype for battery charger is constructed and tested to validate this proposal. Finally, the conclusion is drawn in Section V.

II. Fundamental Analysis

A typical wireless battery charging system consists of three stages to charge a battery wirelessly: the inverter stage, the inductive link, and the rectifier stage. In the following paper, the lowercase letters are used for the representation of instantaneous signal which varies with time, dc value and rms value are denoted by uppercase letters, signals in S-domain are denoted by uppercase letters with a dot on the head of the letter. For example, in Fig. 3, the inverter stage is modeled as an ac voltage source represented by $\dot{V}_1$, whose amplitude is V_1, the rectifier stage is modeled with a pure ac resistive R_{Leq}, and the coil link is modeled as a transformer with a turn ratio equals n. L_1 and L_2 are the self-inductance of the transmitting and receiving coils, whose parasitic resistances are R_1 and R_2, respectively. V_L, R_L and P_{out} denote the output voltage, output load resistance and output power, respectively. To distinguish parameters in the proposed ICCDR system from that in the traditional full-bridge rectifier system, the letters in the traditional rectifier system are with prime symbol (´).

A. Review of S-S WPT Model Working as Voltage Source

The selected WPT topology is a series-series resonant network behaving as a voltage source. The main reasons for this decision are: zero voltage switching (ZVS) behavior in the inverter stage along the whole operating frequency range and the requirement of regulating under a wide power range. In [12], different compensation approaches are analyzed, identifying these advantages in the series-series resonant network behaving as a voltage source. The compensation capacitors placed in series with the coils are tuned with the leakage inductance as in [12], by doing so, it is possible to achieve a constant voltage source.It is worth noting that the ICCDR can be used in different compensation approaches of a S-S WPT system (current source or voltage source).

Thus, the primary and secondary capacitor at the resonant switching angular frequency ω_{res} are selected to satisfy with:

$$C_1 = \frac{1}{\omega_{res}^2 L_1(1-k)} \tag{1}$$

$$C_2 = \frac{1}{\omega_{res}^2 L_2(1-k)} \tag{2}$$

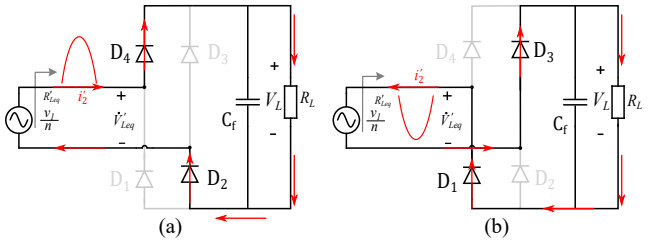

Fig. 4. Equivalent secondary circuit of WPT system based on traditional full bridge rectifier model with diodes. (a) D2 is ON. (b) D1 is ON.

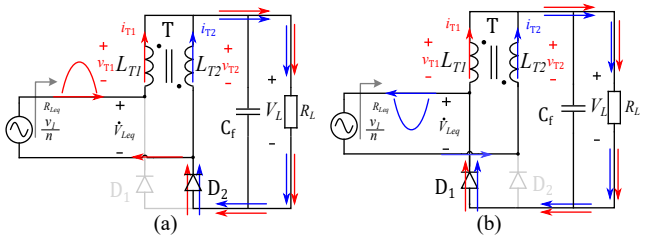

Fig. 5. Equivalent secondary circuit of the proposed WPT system based on ICCDR. (a) D2 is ON. (b) D1 is ON.

Therefore, the impedances $j\omega_{res}L_1(1-k)$ and $j\omega_{res}L_2(1-k)$, cancel with $1/j\omega_{res}C_1$ and $1/j\omega_{res}C_2$ respectively, working as a short circuit at resonance frequency, as shown in Fig. 3.

To obtain a simplified expression of the output voltage gain, the resistances of the non-ideal coils (R_1 and R_2) are neglected since the voltage fall is small. It follows that the output voltage depends on primary ac voltage V_1 and the inductive link turns-ratio n:

$$V_{Leq} = \frac{V_1}{n} \,||\, @\omega_{res} \tag{3}$$

where n is defined as:

$$n = \sqrt{L_1/L_2} \tag{4}$$

Equation (4) is obtained by neglecting the voltage drop on the parasitic resistance of the coils since it is small compared to the input and output voltage. Assuming this simplification and following the methodology proposed in [12], the optimum value of L_2 to achieve the maximum possible efficiency is the matching of the receiver coil self-inductance L_2 to the equivalent ac load resistance R_{Leq}:

$$L_2 = \frac{R_{Leq}}{\omega_{res}k\sqrt{2}} \tag{5}$$

Where k is the coupling factor of the coil link. The maximum efficiency of the coil link is derived as:

$$V_{Leq} = 1 - \frac{2\sqrt{2}}{kQ} \,||\, @\omega_{res} \tag{6}$$

Where Q is the quality factor of the coil, defined as:

$$Q = \frac{\omega_{res}L_1}{R_1} = \frac{\omega_{res}L_2}{R_2} \tag{7}$$

B. Traditional Full Bridge Rectifier

Fig. 4 shows the full bridge rectifier model with diodes for the output. Numbers of publications to derive this model in literature have been analyzed [29]. With the first harmonic approximation, a resistive load with a diode rectifier and a capacitive output filter operating at a constant output power P_{out} and output voltage V_L can be modeled by the equivalent ac resistance R'_{Leq}, which can be derived as:

$$R'_{Leq} = \frac{8}{\pi^2}R_L = \frac{8}{\pi^2}\frac{V_L^2}{P_{out}} \tag{8}$$

From (5) and (8), the designed secondary coil self-inductance for the traditional rectifier system is derived as:

$$L'_2 = \frac{8R_L}{\sqrt{2}\pi^2 k\omega_{res}} \tag{9}$$

With the first harmonic approximation, the turn ratio in the traditional rectifier system is derived from (3):

$$n' = \frac{V_{IN}}{V_L} \tag{10}$$

With (4), (8), (9), and (10), the primary coil self-inductance is expressed as:

$$L'_1 = \frac{8V_{IN}^2}{\sqrt{2}\pi^2 k\omega_{res}P_{out}} \tag{11}$$

C. Inverse Coupled Current Doubler Rectifier

In Fig. 5, the secondary ICCDR circuit is shown, which consists of an autotransformer T (an inverse coupled 1:1 transformer) and two diodes, where these two diodes can be substituted by two grounded synchronous rectifier switches to strongly reduce the losses. The two windings of the auto-transformer continuously fed the output, while the two diodes conduct complementarily. The current through the secondary coil is half of the load current, which is good for high current low voltage applications. L_{T1} and L_{T2} represent the primary and secondary magnetizing inductance of the transformer, respectively. Unlike the traditional CDR with two output inductors which will change the current in the secondary coil, the proposed ICCDR does not change the characteristic of the series resonant in the secondary.

v_{T1} and v_{T2} are the primary and secondary voltage across the transformer windings. i_{T1} and i_{T2} are the current through the windings, respectively. The coupling coefficient k_T and mutual inductance M_T of the autotransformer in the ICCDR are defined as:

$$k_T = \frac{M_T}{\sqrt{L_{T1}L_{T2}}} \tag{12}$$

The ICCDR operates as following:

When the secondary current is positive [shown in Fig. 5 (a)], D_2 is turned on, half of the load current in D_1 circulate directly though winding 2 of the autotransformer back to the load, which is shown with blue arrows in Fig. 5 (a), the other half (arrows in red) goes to the secondary coil and back to the load through transformer winding 1.

When D_2 is conducting, the voltage of autotransformer winding 2 equals output voltage V_L, as shown in Fig. 6 (b). All the simulations in this paper are based on the nominal condition (10kW, 48V) without considering the parasitic.

The equations of the transformer winding are expressed as:

$$v_{T1}(t) = -L_{T1}\left(\frac{di_{T1}}{dt}\right) + M_T\left(\frac{di_{T2}}{dt}\right) \tag{13}$$

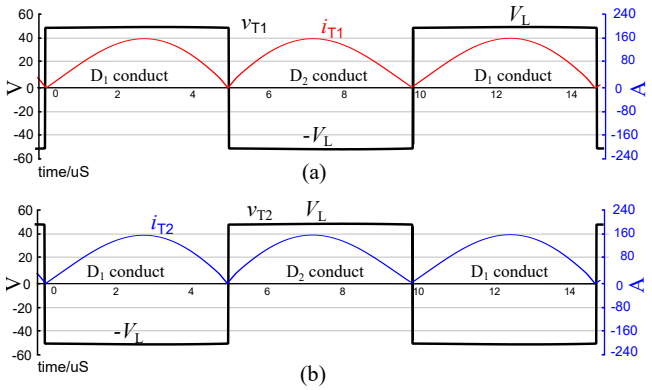

Fig. 6. Simulated waveforms in the autotransformer of the ICCDR at nominal power (10kW, 48V). (a) Current and voltage through winding 1. (b) Current and voltage through winding 2.

$$v_{T2}(t) = -L_{T2}\left(\frac{di_{T2}}{dt}\right) + M_T\left(\frac{di_{T1}}{dt}\right) = V_L \tag{14}$$

According to Kirchhoff´s Voltage Law (KVL), the equivalent output voltage is derived as:

$$v_{Leq} = -v_{T1} + V_L \tag{15}$$

In the 1:1 autotransformer, the primary and secondary inductance equal:

$$L_{T1} = L_{T2} \tag{16}$$

With (13), (14), (15) and (16) the equivalent output voltage when D_2 is turned on can be expressed as:

$$v_{Leq} = (1 - k_T^2)L_{T1}\left(\frac{di_{T1}}{dt}\right) + (1 + k_T)\,V_L \tag{17}$$

If it is assumed the 1:1 transformer is ideal, the coupling coefficient k_T is equal to 1, the voltage across winding 1 equal -V_L, where the waveform is shown in Fig. 6 (a). When D_2 is turned on v_{Leq}(t) can be expressed as:

$$v_{Leq} = 2V_L \tag{18}$$

Similarly, in Fig. 5 (b), when the secondary coil current is negative, D_2 is turned off and D_1 conducts. Half of the load current in D_1 goes through winding 1 directly back to the load, the red arrows in Fig. 5 (b) show the circulation path, the other half of the current in D_1 will go back to the secondary coil L_2 first, then go back to the load through winding 2 of the transformer.

Using the same method, during D_1 is on, v_{Leq} can be expressed as:

$$v_{Leq} = -2V_L \tag{19}$$

Equation (18) and (19) show that the ICCDR performs like a voltage source as a normal full bridge rectifier does; both rectifiers apply a square ac voltage to the resonant link receiver that is compatible with the current source behavior of the series-series resonant link that imposes a sinusoidal current. On the other hand, the traditional CDR imposes an ac square current waveform.

It can be confirmed that the amplitude of v_{Leq} is twice of output voltage V_L. While the current in the secondary coil is half of the output current. The rectified tank output current, $2|i_2(t)|$, is filtered by capacitor C_f. Since no dc current can pass through C_f, the dc component of $2|i_2(t)|$ must be equal to the steady-state load current I_L. By equating dc components, it is obtained:

$$I_L = \frac{2}{T_s}\int_0^{T_s/2} 2\,|i_2(t)|\,dt = \frac{4}{\pi}I_2 \tag{20}$$

Where I_2 is the amplitude of i_2(t). Since the fundamental component of v_{Leq}(t) is in phase with i_2(t). Based on first harmonic approximation method [29] the ICCDR can be modeled as a pure resistive load R_{Leq}:

$$R_{Leq} = \frac{v_{Leq}(t)}{i_2(t)} = \frac{8V_L/\pi}{\pi I_L/4} = \frac{32}{\pi^2}R_L \tag{21}$$

Where the equivalent ac resistance of the ICCDR is 4 times of the resistance in the conventional rectifier under the same specification.

Thanks to the equivalent ac load changing, the secondary coil inductance needed in the proposed WPT system with ICCDR should be 4 times of that in the traditional full bridge rectifier to keep the same behavior in primary, which can be derived as:

$$L_2 = \frac{32R_L}{\sqrt{2}\pi^2 k\omega_{res}} = 4L_2^{'} \tag{22}$$

It means the resonant secondary capacitance needed is 4 times smaller. In high power and high output current applications, the secondary coil self-inductance value needed is lower, being more sensitive to the coil geometry and tolerance and parasitic inductance due to external connections between the secondary coil and the resonant capacitors. However, the higher inductance needed in the ICCDR will be less sensitive.

With (18), (19), and (3) the turn ratio in the proposed WPT system is derived as:

$$n = \frac{V_{IN}}{2V_L} = \frac{n^{'}}{2} \tag{23}$$

With (4), (21), (22), and (23) the primary coil inductance in the proposed WPT system is derived as:

$$L_1 = \frac{8V_{IN}^2}{\sqrt{2}\pi^2 k\omega_{res}P_{out}} = L_1^{'} \tag{24}$$

which is the same with the inductance in the traditional system.

All above, in Table I, a comparison of the secondary side ac current and voltage related with the load dc voltage V_L and load dc current I_L is shown. As demonstrated in Fig. 5,

TABLE I
CURRENT AND VOLTAGE COMPARISON ON THE SECONDARY SIDE

Symbol	Quantity	Full bridge rectifier	ICCDR
I_2 (rms)	Current through secondary coil	$\frac{\pi}{2\sqrt{2}}I_L$	$\frac{\pi}{4\sqrt{2}}I_L$
I_D (rms)	Current through diode	$\frac{\pi}{4\sqrt{2}}I_L$	$\frac{\pi}{4\sqrt{2}}I_L$
I_{T1}, I_{T2} (rms)	Current through transformer winding	–	$\frac{\pi}{4\sqrt{2}}I_L$
V_D	Voltage rating on the diode	V_L	$2V_L$

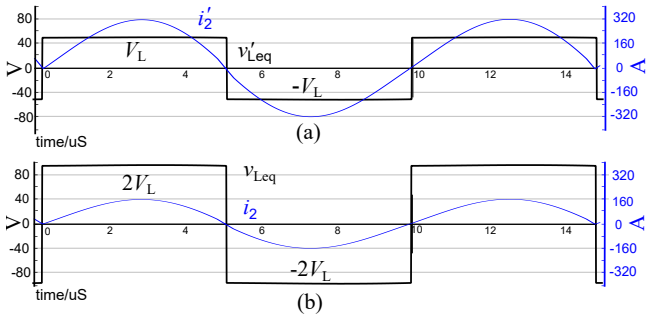

Fig. 7. A comparison of the simulated secondary ac current and voltage waveforms in both systems. (a) Traditional full bridge rectifier WPT system. (b) The proposed ICCDR WPT system.

the whole load current goes through the diode, while only half circulates though the secondary coil. Therefore, with the same design specification (same output voltage and output current), the amplitude of the current through the secondary coil in the proposed system is half of which in the traditional full bridge rectifier system while the amplitude of the square voltage is doubled. The simulated waveform comparison of ac voltage and coil current on secondary side is depicted in Fig. 7. As a result, the equivalent ac resistance load will be 4 times of that with traditional full bridge rectifier which shows agreement with the theoretical analysis in (21). Therefore, if using the ICCDR instead of full bridge rectification and keeping the same design specifications, the secondary coil inductance needed in the proposed system should be 4 times of that needed in the traditional system. If the designed secondary coil in the ICCDR has the double number of turns than that in the full bridge rectifier and keep the same area, the coupling factor will be the same since the coupling factor is only related with the geometry of the coil. Keeping these two design considerations, the primary behavior (voltage and current waveforms, phase shift and ZVS) is the same for both rectifier systems.

III. Converter Design and Comparison

In this section, a detailed design and comparison between the WPT converter with traditional diode rectifier and that with the proposed ICCDR configuration is described. A losses comparison between ICCDR and traditional diode rectifier is analyzed theoretically. A 10kW WPT system with the proposed ICCDR and diodes rectifier is designed and compared. The designed system working frequency is 100kHz. The input voltage of this system is 400V. The output voltage is in the range between 38 Vdc and 55 Vdc, the nominal output voltage is 48V and the rated output current is around 200A. Using the methodology described in Section II-C, the deigned parameters for the traditional WPT system and the WPT with proposed ICCDR can be derived. To make a trade-off between the coil link efficiency and the inverter losses, the designed power is for 7.5kW with an estimated couplings factor 0.42. In Table II, a comparison of designed parameters between the proposed WPT system and the WPT system with traditional rectifier is shown. With the same specification, the voltages and currents remain unchanged on the primary side, regardless of using

TABLE II
Main Parameters Design Comparison for Resonant Link

Quantity	System with full bridge rectifier		System with ICCDR	
Primary coil inductance	L_1'	43 uH	L_1	43 uH
Primary resonant capacitance	C_1'	91.7 nF	C_1	91.7 nF
Secondary coil inductance	L_2'	0.87 uH	L_2	3.5 uH
Secondary resonant capacitance	C_2'	4.08 uF	C_2	1.02 uF

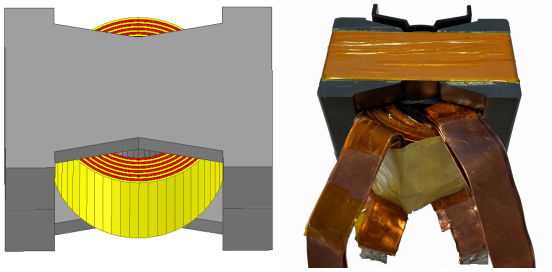

Fig. 8. The autotransformer design in the ICCDR.

TABLE III
Specification of the Autotransformer in ICCDR

Quantity	Value
Core/material	PQ50/50 / 3C95
Foil / width (thickness)	Copper /300 um
Foil / height	Copper /30 mm
Insulator /width (thickness)	Capton / 70 um
Winding ac resistance (100kHz)	0.58 mΩ
Magnetizing inductance	80 uH
Number of turns	3
Number of parallel	2
Leakage inductance	150 nH
Coupling factor	99.81%

the proposed ICCDR. The parameters of the primary coil and primary resonant capacitor keep the same with traditional rectifier. However, this is not true for the secondary side. Table I shows that the secondary coil rms current is reduced by 50%. The diode and output capacitor currents remain unchanged for the converter with an ideally coupled transformer for the proposed ICCDR.

A. Comparison of the Losses in the ICCDR and Full Bridge Rectifier with Diodes

In low output voltage and high output current applications, a big part of losses is wasted on the rectifier stage due to the conduction losses on the components of the rectifier, saving a big amount of energy in the proposed ICCDR compared to the diode-rectifier. Whereas the volume of the proposed ICCDR does not increase compared with the traditional CDR using two inductors.

An interleaved foil transformer is designed to minimize the leakage inductance, which is suitable for high output current

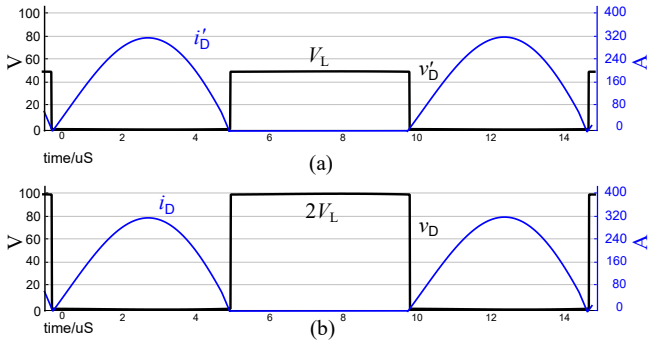

Fig. 9. A comparison of the simulated current and voltage through the semiconductors in both rectifiers. (a) Traditional full bridge rectifier. (b) The ICCDR.

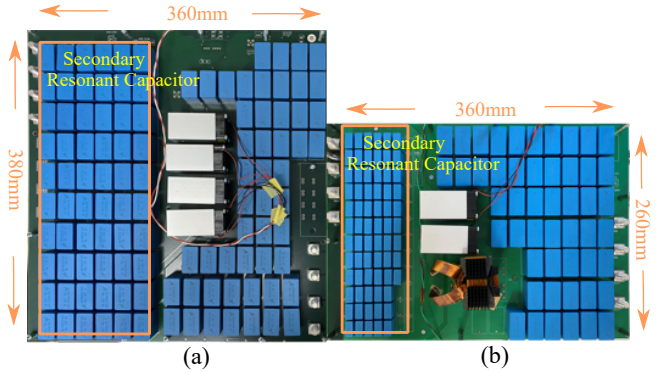

Fig. 10. Prototype of secondary comparison. (a) Full bridge rectifier system. (b) The proposed ICCDR system.

applications. The specification and design parameters of the transformer in ICCDR is shown in Table III. A PQ50/50 core was selected with a good trade-off between the size and losses. The designed transformer has 3 turns with 2 winding in parallel, each winding of primary and secondary is interleaved to reduce the permeability effect and eddy-current effect. The simulation model is built in ANSYS which is shown in Fig. 8. The red winding is primary and yellow one is secondary, which are interleaved. The measured autotransformer parameters are shown in Table III. The currents circulating through the transformer winding are shown in Fig. 6. The voltage across the transformer winding v_{T1} and v_{T2} at worst cases is a square voltage with an amplitude of 55V. The peak ac flux density can be derived [29]:

$$\Delta B = \frac{\lambda}{2nA_e} = 0.14 \text{ T} \tag{25}$$

Where λ denotes the volt-seconds applied during the positive portion of v_{T1} or v_{T2}, A_e is the core effective (cross-sectional) area. According to the datasheet from the core manufacture, the core losses working at 100 kHz can be calculated:

$$P_{core} = 14.8 * \Delta B^{2.55} A_e l_e = 3.63 \text{ W} \tag{26}$$

Where l_e is the core effective length. Based on the FEA model [30], the winding losses contains dc winding losses $P_{dc\_winding}$ and ac winding losses $P_{ac\_winding}$ which are 5.21W and 2.1W, respectively. So, the total losses on the transformer are around 11W.

In Fig. 9, a comparison of the simulated current and voltage though the semiconductors in both rectifiers is shown. The currents trough the semiconductors in both rectifiers are the same, while the voltage withstand by the semiconductors is doubled in the proposed ICCDR. This is one drawback of the proposal. In order to fast validate this proposal, a passive rectifier with diodes in the proposed ICCDR is used.

The diode losses are dominated by the high current (200A) conduction losses as Schottky diodes are used. So, the losses on each diode will be similar for different volage rating. The diode chosen for the proposed ICCDR and the conventional WPT system with diodes rectifier are STPS200170tv1. Fig. 9 shows the waveforms of the current through the diode for 10kW. According to the datasheet given by the diode manufacturer, there is around 85W losses on each diode when 100A average current goes through this diode. The traditional rectifier presents 2 diodes in series while the ICCDR is only 1 diode conducting. By using the proposed ICCDR, 160W losses can be saved, being 47% losses reduction on the rectifier stage. However, it is necessary to highlight that these two diodes in the ICCDR can also be substituted by switches [27], being an active ICCDR.

TABLE IV
COMPARISON OF SECONDARY RESONANT CAPACITOR

Quantity	System with full bridge rectifier	System with ICCDR
rms current (need)	240 A	120 A
rms voltage(need)	77 V	150 V
Capacitor selected	B32654A2683	B32653A2153
Capacitance of each one	68 nF	15 nF
Voltage rating @100 kHz	180 V	350 V
Number of capacitors needed	60	70
Maximum current (rms)	461 A	230 A
Current derating	1.92	1.92
Total Area	6*60 = 360 cm^2	2.9*70 = 203 cm^2
Total Volume	1077 cm^3	418 cm^3

B. Comparison of Secondary Resonant Capacitor

In the high power WPT system, the resonant capacitors account for a huge volume and weight of the whole system. The resonant capacitors are in series with the energy flow, circulating the high secondary resonant current through the corresponding resonant capacitor. In order to do a fair comparison, the capacitors are designed with the same current derating (maximum rated current / maximum circulating current), for the sake of robustness due to the huge circulating currents in secondary the selected current derating is almost 2 (1.92) in both rectifiers. According to (1) and (2), the secondary capacitance needed (1.02uF) in the proposed system is one fourth of that needed (4.08uF) in the traditional full bridge rectifier system, and the amplitude of secondary current circulating through the resonant capacitor is only half of that in the traditional full bridge rectifier system. The rms current through through the secondary resonant capacitor in the proposed

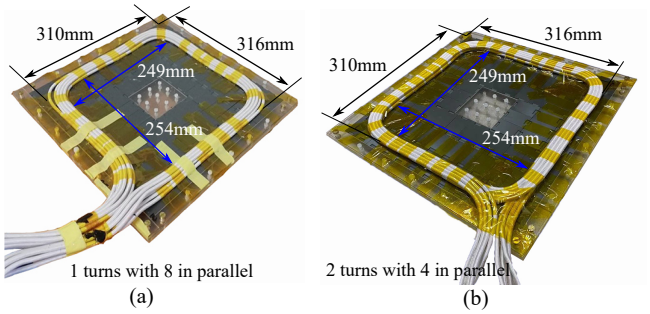

Fig. 11. Designed secondary coil comparison. (a) Secondary coil for full bridge rectifier system. (b) Secondary coil for the proposed system.

TABLE V
PARAMETERS COMPARISON OF COIL LINK

Quantity	System with full bridge rectifier	System with ICCDR
Primary coil inductance	43.7 uH	43 uH
Secondary coil inductance	960 nH	3.53 uH
Primary coil ac resistance	67 mΩ	67.5 mΩ
Secondary coil ac resistance	2.2 mΩ	7.4 mΩ
Voltage rating @100 kHz	180 V	350 V
Distance	40 mm	40 mm
Coupling factor	0.4	0.4

system is 120A, while in the traditional full bridge rectifier system, it is 240A. Based on the design specification, the capacitors selected are shown in Table IV. The capacitor selected for the traditional system is B32654A2683 from TDK, the capacitance is 68nF, and the maximum rms voltage at 100kHz is 180V, 60 parallel capacitors are needed to achieve 4.08uF. The designed resonant capacitor for the proposed system has 60 parallel 15nF capacitors (B32653A2153) to obtain 1.02uF of capacitance with 350V maximum voltage rating at 100kHz. The obtained voltage derating (maximum rated voltage / maximum applied voltage) is very similar, about 1.65 in both rectifiers. Keeping the same ac current derating and the same ac voltage derating, the secondary resonant capacitors of the ICCDR system have an area 43% lower and a volume 61% smaller than those of the full bridge system.

C. Comparison of Secondary Coil

The inductance needed in the secondary coil for the proposed system system is 4 times larger than that needed in the diode-rectifier full bridge rectifier system, having the double number of turns in the ICCDR than in the full bridge rectifier to keep the same specification in both systems. The methodology followed to design the coil link is the one proposed in [30]. Since the coupling factor is only related with the geometry of the coils, the secondary coil is designed to have the same area in both rectifier systems to have the same coupling factor, being a fair comparison of the system efficiency (not influenced by the coupling factor difference). Therefore, the designed secondary coil for the full bridge rectifier system has 1 turn with 8 in parallel, which is shown in

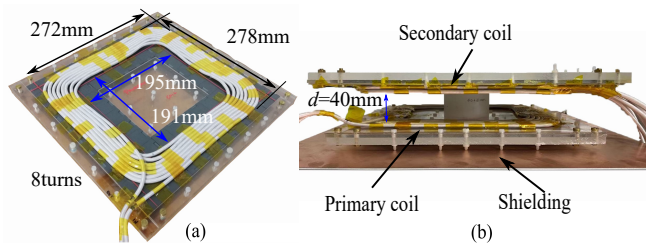

Fig. 12. Prototype of primary coil and coil alignment. (a) Primary coil geometry. (b) Coil alignment.

Fig. 11 (a). As a comparison, the designed secondary coil for the proposed system is shown in Fig. 11 (b), which has 2 turns with 4 in parallel and the inductance increased 4 times. The size and weight of these two coils is similar and the increased inductance in the proposed system does not introduce more volume and weight to the system. Table V shows the measured coils inductance and coupling factor. With 2 turns instead of 1 turn for the secondary, the coupling factor almost keeps the same, which means that the main characteristic of the inductive link is same to do a fair comparison between both rectifier circuits.

To have a fair comparison everything is the same in primary, the coupling is the same and the differences are only in the secondary, having the same specifications. The primary coil, primary resonant capacitors and inverter keep using the same in both rectifier WPT systems. However, the proposed system can save about 160W losses in the proposed ICCDR when delivering 10kW, and the power density can be increased dramatically by the new configuration of the secondary resonant capacitor.

IV. EXPERIMENTAL VALIDATION

In order to verify the proposal, a 10kW WPT system with 400V input and 48V output voltage is developed. The primary coil and coil link alignment are shown in Fig. 12 (b). The selected switches in the inverter stage are SiC MOSFET (C3M0030090K) since they present very good features to be employed in this sort of application. Two MOSFETs are mounted in parallel, one is on the top side the other is on the bottom side, to reduce the conduction losses. In addition, a heat-sink with an integrated fan is included to help the dissipation. The designed primary coil that has 8 turns in one layer is shown in Fig. 12 (a), which presents 43.7uH inductance. The experimental setup to test the 10kW WPT system is shown in Fig. 13. The microcontroller to generate the control signals is TMS320F28379D from Texas Instruments. The main parameters of the system are shown in Table VI.

Fig. 14 shows the main waveforms of the proposed WPT system operating at rated power. In Fig. 14 (a), the square input voltage and primary coil current are depicted. It can be observed that the primary coil current i_1 is still sinusoidal and the proposed ICCDR has no impact on the primary circuit behavior. Fig. 14 (b) shows the current through the primary winding of the autotransformer in the proposed ICCDR and the voltage across D_1. The peak-to-peak current is 160A, continuously feeding the output. The secondary winding current is just

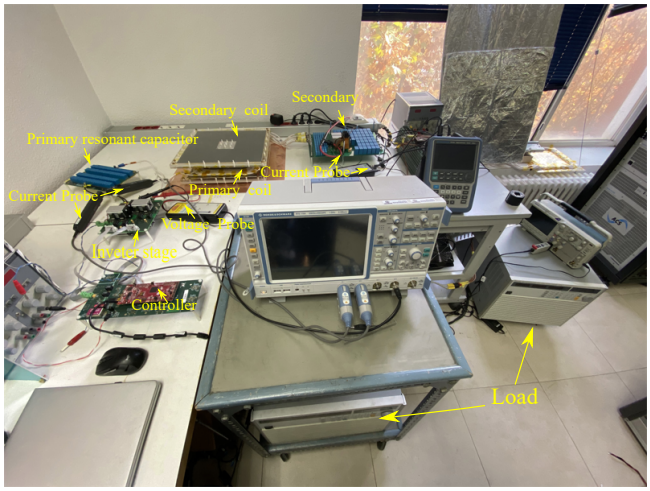

Fig. 13. Experimental setup.

TABLE VI
MAIN PARAMETERS OF THE SYSTEM

Symbol	Quantity	Value
V_{IN}	Input voltage	400 V
V_L	Nominal output voltage	48 V
P_{out}	Nominal output power	10 kW
f_{res}	Nominal frequency	100 kHz
L_1	Primary coil inductance	43.7 uH
L_2	Secondary coil inductance	3.55 uH
d	Distance	40 mm
k	Coupling factor	0.4
C_1	Nominal primary capacitance	93 nF
C_2	Nominal secondary capacitance	1.02 uF
Q_1-Q_4	MOSFET	C3M0030090K
D_1-D_2	Diodes	STPS200170tv1

the same than the primary one. The output current before the output capacitor will double, being a rectified sine wave with an amplitude of 320A, which means the average output current circulating though the load is around 200A. One drawback of this proposed circuit is the voltage ringing on the diodes, which can be observed in Fig. 14 (b). This ringing is caused by the leakage inductance of the autotransformer and the parasitic elements in the circuit. To damp this ringing a snuber circuit is needed to prevent from damaging the components. In [31], two passive lossless snubber circuits are proposed for current doubler refctifiers, which could be used in the ICCDR to damp the ringing, it can recycle the energy stored in the leakage inductance.

In Fig. 15, the loss breakdown at a nominal output power (10kW) is shown. It can be seen that the efficiency is mainly influenced by the power semiconductors (diodes and MOSFETs) and the coil link. Due to the compensation approach working as a voltage source, the primary MOSFETs can achieve ZVS, and the switching losses are small (40W) compared with the conduction losses (88W), with two MOSFET in parallel. Even though we only have two diodes instead of four,

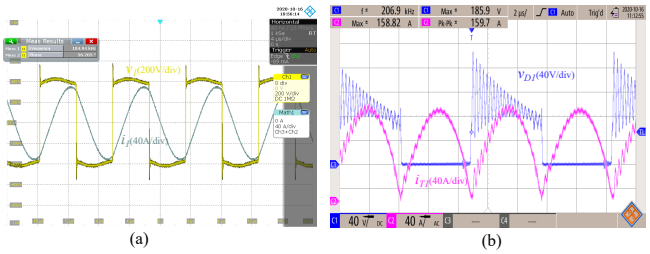

Fig. 14. Main waveforms of the experimental results. (a) Square input voltage and Primary coil current. (b) The voltage of D_1 and current of transformer winding 1.

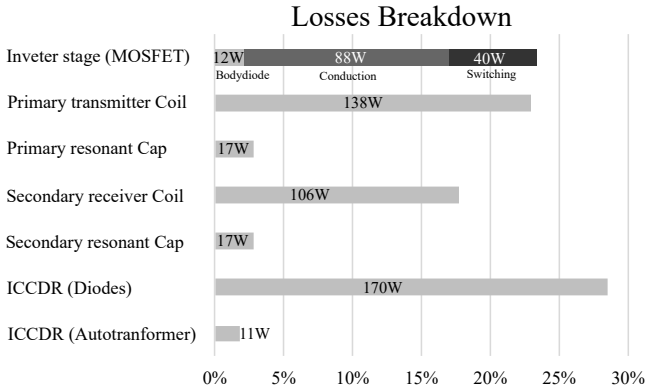

Fig. 15. Estimated losses breakdown at nominal output power.

the losses on the diodes in ICCDR still accounts for a big part of the losses of the whole system due to the forward voltage drop of the diodes. But 47% losses on the rectifier stage can be saved compared with the traditional four diodes rectifier. Synchronous rectification could reduce the conduction losses, especially when paralleling the rectifier switches. These two diodes in ICCDR can be substituted by two grounded switches, becoming to an active rectifier. Even though, the impact is not significant than the passive rectifiers, there are still 27% losses reduction when the active ICCDR is used compared with the full bridge active rectifier (with MOSFETs).

In Fig. 16, the comparison of the measured frequency response to the voltage gain is shown. Three different loads (0.275Ω, 0.75Ω, 2.3Ω) are described to show the impact of the proposed circuit to the frequency response. The gain characteristic of the proposed system and the traditional diode-rectifier system shows great agreement. In the nominal load condition (0.275Ω), the voltage gain of the proposed ICCDR system (red dash lines) is around 2V higher than that of the traditional diode-rectifier system (red solid lines), which is caused by the voltage fall of the extra two diodes in the traditional system and the tolerance of the system but being within the expectation. It can be observed this difference reduces with the decrease of the load. It can be validated that the proposed system does not change the behavior of the circuit and the same control strategy can be used in the proposed ICCDR WPT system.

The total efficiency and losses comparison are presented in Fig. 17 for different load conditions (4.6Ω, 2.3Ω, 1.15Ω, 0.75Ω, 0.5Ω, 0.575Ω, 0.45Ω, 0.385Ω, 0.33Ω, 0.275Ω) with the

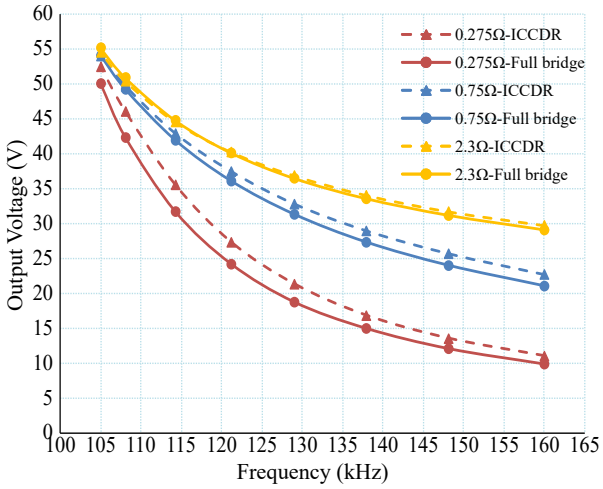

Fig. 16. Comparison of voltage gains.

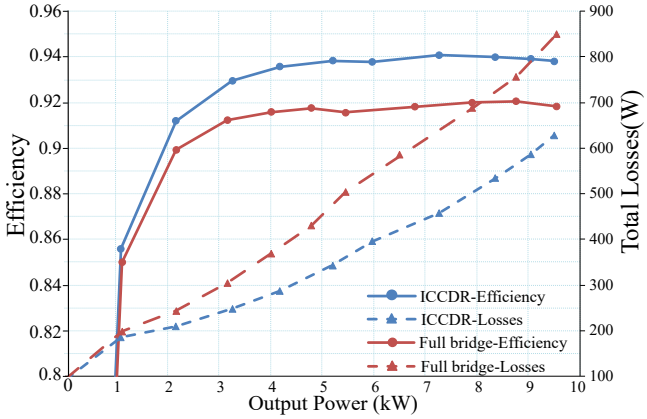

Fig. 17. Comparison of the losses and efficiency.

fixed nominal frequency and the change of load resistance. The efficiency curve of the proposed ICCDR system is depicted with blue lines with a peak efficiency of 94.07% at 7.2kW, the red lines denote the traditional diode-rectifier system with a peak efficiency of 92.06% at 8.7kW. 2% efficiency is improved, and 220 W energy is saved in the proposed system when the delivered power is 9.5kW.

It is shown that the analysis and measurements are in good agreement. Additionally, it is validated that the proposed ICCDR WPT system does not have effect on the gain characteristics of the system and does not change the primary circuit behavior in terms of the primary current, voltage and circuit parameters. Besides, the efficiency of the proposed system improved 2% compared to the diode-rectifier system.

V. Conclusion

In this paper, a 10-kW 400V/48V wireless power transfer (WPT) system with an inverse coupled current-doubler rectifier (ICCDR) is presented. The ICCDR consists of an autotransformer and two diodes instead of four diodes to reduce the losses on the didoes for high current low voltage WPT applications. In the proposed WPT system based on ICCDR, the current though the secondary coil reduces half, the secondary resonant capacitor value is one fourth of the traditional system.

A detailed comparison between the proposed system and full bridge rectifier system is presented. Both systems (the proposed ICCDR system and the traditional diode-rectifier system) are constructed experimentally with the same specifications to compare the results and validate the proposal. An overall efficiency of 94% is achieved in the proposed system. Experimental results show that a 2% efficiency is improved in the proposed system with 220W energy saved when delivering 9.5kW output power. It has been validated that the proposed ICCDR does not change the system's frequency response of voltage gain and the design parameters of primary keep the same. However, the configuration of the secondary resonant capacitor will change, leading to a 43% area saving and 61% volume reduction on the secondary resonant capacitors under the same design specification. The system efficiency and power density are improved significantly in the proposed system.

The two diodes in the proposed ICCDR can be substituted by two grounded switches to strongly reduce the power losses on the rectifier. The drawback of the proposed system is the voltage ringing on the diodes, which is caused by the leakage inductance of the autotransformer and the parasitic resonance between the capacitance in the circuit. This ringing can be reduced by using the lossless passive snubber proposed in [31]. A WPT system based on ICCDR is a very appropriate topology for high power and high current applications. The proposed solution should be a good candidate for fast wireless battery chargers.

References

[1] C. Xiao, K. Wei, D. Cheng and Y. Liu, "Wireless Charging System Considering Eddy Current in Cardiac Pacemaker Shell: Theoretical Modeling, Experiments, and Safety Simulations," *IEEE Trans. Ind. Electron.*, vol. 64, no. 5, pp. 3978-3988, May 2017.

[2] D. Ahn and S. Hong, "Wireless Power Transmission with Self-Regulated Output Voltage for Biomedical Implant," *IEEE Trans. Ind. Electron.*, vol. 61, no. 5, pp. 2225-2235, May 2014.

[3] D. Kim and D. Ahn, "Self-Tuning LCC Inverter Using PWM-Controlled Switched Capacitor for Inductive Wireless Power Transfer," *IEEE Trans. Ind. Electron.*, vol. 66, no. 5, pp. 3983-3992, May 2019.

[4] L. Shi, J. C. Rodriguezt and P. Alou, "Modeling and Analysis of Total Harmonic Distortion in Series-Series Wireless Power Transfer System for 6.78 MHz," *IEEE Energy Conversion Conf. and Expo. (ECCE)*, Detroit, MI, USA, 2020, pp. 1016-1020.

[5] L. Shi, P. Alou, J. A. Oliver, and J. A. Cobos, "A Novel Self-Adaptive Wireless Power Transfer System to Cancel the Reactance of the Series Resonant Tank and Deliver More Power," *IEEE Energy Conversion Conf. and Expo. (ECCE)*, Baltimore, MD, USA, 2019, pp. 4207-4211.

[6] M. Borage, S. Tiwari, and S. Kotaiah, "Analysis and design of an LCL-T resonant converter as a constant-current power supply," *IEEE Trans. Ind. Electron.*, vol. 52, no. 6, pp. 1547-1554, Dec. 2005,

[7] S. Y. R. Hui, W. Zhong and C. K. Lee, "A Critical Review of Recent Progress in Mid-Range Wireless Power Transfer," *IEEE Trans. Power Electron.*, vol. 29, no. 9, pp. 4500-4511, Sept. 2014.

[8] A. Namadmalan, "Bidirectional Current-Fed Resonant Inverter for Contactless Energy Transfer Systems," *IEEE Trans. Ind. Electron.*, vol. 62, no. 1, pp. 238-245, Jan. 2015.

[9] H. Tebianian, Y. Salami, B. Jeyasurya and J. E. Quaicoe, "A 13.56-MHz Full-Bridge Class-D ZVS Inverter With Dynamic Dead-Time Control for Wireless Power Transfer Systems," *IEEE Trans. Power Electron.*, vol. 67, no. 2, pp. 1487-1497, Feb. 2020.

[10] S. Samanta, A. K. Rathore and D. J. Thrimawithana, "Analysis and Design of Current-Fed Half-Bridge (C)(LC)-(LC) Resonant Topology for Inductive Wireless Power Transfer Application," *IEEE Trans. Ind. App.*, vol. 53, no. 4, pp. 3917-3926, July-Aug. 2017,
[11] A. T. L. Lee, W. Jin, S. Tan and S. Y. Hui, "Buck-Boost Single-Inductor Multiple-Output High-Frequency Inverters for Medium-Power Wireless Power Transfer," *IEEE Trans. Power Electron.*, vol. 34, no. 4, pp. 3457-3473, April 2019.
[12] A. Delgado, N. A. Requena, R. Ramos, J. A. Oliver, P. Alou and J. A. Cobos, "Design of Inductive Power Transfer System With a Behavior of Voltage Source in Open-Loop Considering Wide Mutual Inductance Variation," *IEEE Trans. Power Electron.*, vol. 35, no. 11, pp. 11453-11462, Nov. 2020.
[13] Chwei-Sen Wang, O. H. Stielau, and G. A. Covic, "Design considerations for a contactless electric vehicle battery charger," *IEEE Trans. Power Electron.*, vol. 52, no. 5, pp. 1308-1314, Oct. 2005.
[14] W. Zhang, S. Wong, C. K. Tse and Q. Chen, "Analysis and Comparison of Secondary Series- and Parallel-Compensated Inductive Power Transfer Systems Operating for Optimal Efficiency and Load-Independent Voltage-Transfer Ratio," *IEEE Trans. Power Electron.*, vol. 29, no. 6, pp. 2979-2990, June 2014.
[15] W. Zhang and C. C. Mi, "Compensation Topologies of High-Power Wireless Power Transfer Systems," *IEEE Trans. Veh. Technol.*, vol. 65, no. 6, pp. 4768-4778, June 2016,
[16] M. Borage, S. Tiwari and S. Kotaiah, "Analysis and design of an LCL-T resonant converter as a constant-current power supply," *IEEE Trans. Ind. Electron.*, vol. 52, no. 6, pp. 1547-1554, Dec. 2005.
[17] S. Zhou and C. Chris Mi, "Multi-Paralleled LCC Reactive Power Compensation Networks and Their Tuning Method for Electric Vehicle Dynamic Wireless Charging," *IEEE Trans. Ind. Electron.*, vol. 63, no. 10, pp. 6546-6556, Oct. 2016.
[18] A. Berger, M. Agostinelli, S. Vesti, J. A. Oliver, J. A. Cobos, and M. Huemer, "A wireless charging system applying phase-shift and amplitude control to maximize efficiency and extractable power," *IEEE Trans. Power Electron.*, vol. 30, no. 11, pp. 6338-6348, Nov. 2015.
[19] T.F. Wu, C.T. Tsai, Y.D. Chang, and Y.M. Chen, "Analysis and implementation of an improved current-doubler rectifier with coupled inductors," *IEEE Trans. Power Electron.*, vol. 23, no. 6, pp. 2681-2693, 2008.
[20] U. Badstuebner, J. Biela, D. Christen, and J. W. Kolar, "Optimization of a 5-kW Telecom Phase-Shift DC-DC Converter With Magnetically Integrated Current Doubler," *IEEE Trans. Ind. Electron.*, vol. 58, no. 10, pp. 4736-4745, Oct. 2011,
[21] Huang-Jen Chiu and Li-Wei Lin, "A high-efficiency soft-switched AC/DC converter with current-doubler synchronous rectification," *IEEE Trans. Ind. Electron.*, vol. 52, no. 3, pp. 709-718, June 2005.
[22] J. Kim, I. Lee, and G. Moon, "Integrated Dual Full-Bridge Converter with Current-Doubler Rectifier for EV Charger," *IEEE Trans. Power Electron.*, vol. 31, no. 2, pp. 942-951, Feb. 2016.
[23] K. Huang, H. Hsieh and R. Wai, "Phase-Shifted Full-Bridge Converter for a Half-Current-Multiplier Rectifier Using an Autotransformer-Based Filter," *IEEE Trans. Transp. Electrific.*, vol. 6, no. 1, pp. 199-212, March 2020.
[24] P. Alou, J. A. Oliver, O. Garcia, R. Prieto and J. A. Cobos, "Comparison of current doubler rectifier and center tapped rectifier for low voltage applications," *IEEE Appl. Power Electron. Conf. and Expo. (APEC)*, 2006, Dallas, TX, USA, 2006, pp. 744 -750.
[25] Y. Zhang and M. d. Rooij, "Rectifier Topology Comparison in 6.78 MHz Highly Resonant Wireless Power Systems," *IEEE Appl. Power Electron. Conf. and Expo. (APEC)*, Anaheim, CA, USA, 2019, pp. 671-677.
[26] Y. Wang et al., "Research on 11kW Wireless Charging System for Electric Vehicle Based on LCC-SP Topology and Current Doubler," *IEEE Energy Conversion Conf. and Expo. (ECCE)*, Detroit, MI, USA, 2020, pp. 820-827.
[27] J.Y. Shin, H.-W. Kim, K.-Y. Cho, S.-S. Hwang, S.-K. Chung and G.-B. Chung, "Analysis of LLC resonant converter with current-doubler rectification circuit," *Proc. 16th Int. Power Electron. Motion Control Conf. Expo.*, pp. 162-167. 2014.
[28] S. Klötzer, F. Thielke, M. Warncke and K. F. Hoffmann, "Analysis of an LLC Converter with Planar Inverse Coupled Current Doubler Rectifier using Silicon and GaN devices," *Proc. EPE*, pp. 1-10, 2019.
[29] R. Erickson and D. Maksimovi, Fundamentals of Power Electronics. Boston, MA, USA: Springer, 2001.
[30] A. Delgado, D. Schoenberger, J. Á. Oliver, P. Alou and J. A. Cobos, "Design Guidelines of Inductive Coils Using a Polymer Bonded Magnetic Composite for Inductive Power Transfer Systems in electric Vehicles," *IEEE Trans. Power Electron.*, vol. 35, no. 8, pp. 7884-7893, Aug. 2020
[31] H. Mao, J. A. Abu-Qahouq, W. Qiu, Y. Wen and I. Batarseh, "Lossless snubber circuits for current doubler rectifiers to reduce reverse-recovery losses," *Proc. 29th IEEE IECON*, vol. 3, pp. 2639-2644, 2003.

Lixin Shi (S'19) was born in Shijiazhuang, China. He received the M.S. degree in electrical engineering from Beijing Jiaotong University (BJTU), Beijing, China in 2016. He is currently working toward the Ph.D. degree in power electronics from 2016 in Universidad Politécnica de Madrid (UPM), Madrid, Spain.

His research interests include wireless power transfer and resonant converters.

Alberto Delgado (S'17) received the B.Sc. degree in electrical engineering from the University of Málaga (UMA), Malaga, Spain, in 2016, and the M.Sc. degree in industrial electronics in 2017 from the Universidad Politécnica de Madrid (UPM), Madrid, Spain, where he is currently working toward the Ph.D. degree in industrial electronics. He became a Teaching Assistant with UPM in 2019.

His research interests include modeling of dc-dc converters for inductive power transfer system, magnetic components for different applications, such as RFID communications and wireless charging, and magnetic nanomaterials and micro-materials.

Regina Ramos (M'21) received the B.Sc. degree in electrical engineering, the M.Sc. degree in industrial electronics, and Ph.D. degree in Electrical and Electronic Engineering in 2014, 2016, and 2021 respectively, from the Universidad Politecnica de Madrid, Madrid, Spain, where she is currently working as teaching assistant.

Her research interests include switching-mode power supplies, power architectures, and digital control applied to power electronics.

Pedro Alou (M'07) was born in Madrid, Spain, in 1970. He received the M.S. and Ph.D. degrees in Electrical Engineering from the Polytechnic University of Madrid (UPM), Spain in 1995 and 2004, respectively. Currently, he is Full Professor in this university. He has been involved in Power Electronics since 1995, participating in more than 70 R&D projects with the industry. He has authored or coauthored over 45 journal articles, 140 conference papers and holds six patents.

His main research interests are in power converters, advanced topologies for efficient energy conversion, modeling of converters and magnetic components, advanced control techniques for high dynamic response, energy management and new semiconductor technologies for power electronics. His research activity is distributed among industrial, aerospace, and military projects.